Journal of Sciences, Islamic Republic of Iran 16(2): 153-168 (2005) http://jsciences.ut.ac.ir
University of Tehran, ISSN 1016-1104

S-C-O Isotopes, Fluid Inclusion Microthermometry, and the Genesis of Ore Bearing Fluids at Qaleh-Zari Fe-Oxide Cu-Au-Ag Mine, Iran

M.H. Karimpour,[1,*] Khin Zaw,[2] and D.L. Huston[3]

[1] *Department of Geology, Faculty of Sciences, Ferdowsi University, Mashhad, Islamic Republic of Iran*
[2] *Centre for Ore Deposit Research, University of Tasmania, Hobart, Tasmania, Australia 7001*
[3] *Australian Geological Survey Organization, Canberra, ACT, Australia 2601*

Abstract

Qaleh-Zari is a Fe-oxide Cu-Ag-Au vein type deposit located 180 km south of Birjand, in eastern Iran. Host rocks are mainly Tertiary calc-alkaline to K-rich calc-alkaline with transition to shoshonitic andesite and andesitic basalts, but in the central part shale and sandstone of Jurassic age. Andesitic rocks from the western region of Qaleh-Zari were dated to 40.5 ± 2 Ma. Four trends of faults and joints are identified in the mine area. Cu-Ag-Au mineralization is present only in the oldest sets of faults and joints that crosscut the Tertiary and Jurassic units. Three major sub-parallel steep quartz veins are identified. No.1 vein is about 650 m long and No.3 vein is less than 500 m long. No.2 vein is traced for more than 3.5 km horizontally along strike (N40° W) and more than 350 m down dip. Specularite and quartz are the most abundant primary oxides. Chalcopyrite is the only hypogene copper mineral. Silver is present as sulfosalt minerals. Paragenesis: Stage I: specularite, quartz, Fe-chlorite, chalcopyrite and sulfosalts. Specularite deposited first and forms 10 to 25 percent of the vein. Stage II: quartz, chalcopyrite, pyrite, chlorite ± hematite ± sulfosalt minerals. Stage III: quartz ± pyrite ± chalcopyrite. Stage IV: hematite, quartz, and ± calcite. The ores grade typically 2-9% Cu, 100-650 ppm Ag, and 0.5-35 ppm Au. Homogenization temperatures of fluid inclusions associated with Cu, Ag, and Au deposition were varying between 360°C and 240°C. The salinity of the fluid was between 1 to 6 wt % NaCl equiv and the CO_2 content was low (less than 1 mole %). The $\delta^{34}S_{CDT}$ values of pyrite and chalcopyrite were between 0.4 to 2.2‰, which was consistent with a magmatic-hydrothermal or leached volcanic source. The $\delta^{13}C_{PDB}$ values of calcite were between 16.9 to 17.4‰ and the calculated $\delta^{13}C_{PDB}$ of the fluid is between −3.8 and −3.0‰. The $\delta^{18}O_{SMOW}$ of the carbonates were between 16.96 and 19.40‰. Calculated fluid $\delta^{18}O_{SMOW}$ values were 7.4 to 9.8‰, which overlapped the range of magmatic water. The C and O isotopic values of calcite were similar to porphyry copper deposits, possibly indicating magmatic affinities for the ore fluids. Based on the presence of hematite, chalcopyrite, Fe-rich chlorite and locally pyrite, and on the absence of magnetite and pyrrhotite, the ore fluid was very oxidized. Oxygen fugacity was estimated to have been between 10^{-27} and 10^{-32}, and the fugacity of H_2S was less than $10^{-3.5}$.

Keywords: Qaleh Zari; C-O isotopes; Fluid inclusion microthermometry; Iran

1. Introduction

The Qaleh-Zari deposit consists of a series of specularite-rich Cu-Au-Ag-bearing vein located 180 km south of Birjand (Province of Khorasan) at an elevation between 1500 to 1600 m. Mining in the Qaleh-Zari area dates back more than 2000 years. Historic mining extended to a depth of 90 m, and historic production is estimated at 0.9 Mt based on the extent of open cavities. The historic miners appear to have the known smelting techniques as old slag dumps and mining tools are recovered in the area. More than 4 million tons of ore

* *E-mail: mhkarimpour@yahoo.com*

have been mined up and it is estimated that there is more than 3 million tons still present in the area. Qaleh-Zari is a high grade Cu-Ag-Au deposit. The ores grade typically 2-9% Cu, 100-650ppm Ag, and 0.5-35ppm Au.

Modern exploration was started by two Iranian and Japanese Nittetsu mining Companies in 1971, and production started in 1975 at rate of 18,000 tons/year with continuous operation for the last 30 years. Only four case of study beside this work have been done at Qaleh-Zari deposit [1-4].

The aims of this study were: 1) to document the geological setting and the geochemical signature of host volcanic sequence, 2) to establish the paragenesis of the deposit, 3) to characterize the ore-bearing fluid, and 4) to document the distribution of ore metals in the deposit.

2. Regional Geology

Qaleh-Zari is situated within the Central Lut Block at 31° 50′ N, 59° 00′ E (Eastern Iran). The Lut Block is essentially a north-south-trending rigid mass smoothly surrounded by ranges of central and eastern Iran (Fig. 1a). The Lut Block extends over 900 km in north-south direction and only 200 km wide in east-west direction. It is confined by Nayband fault and Shotori Range in the west and the Eastern Iranian Ranges in the east (Fig. 1a). The western edge of the Lut Block is cut off by Nayband normal fault. The northern termination of Lut Block is the depression of Kavir-e-Namak and the Great Kavir Fault. The Bazman volcanic complex and the Jaz-Murian-Depression define the southern edge. The eastern edge is dissected by Sistan suture zone (Fig. 1a). The Lut Massif has a relatively low degree of Cretaceous Alpine deformation. Most of the area is covered with Tertiary continental sediments and volcanic rocks with scattered outcrops of Mesozoic and Paleozoic rocks.

The Sistan suture zone extends from Makran in southeastern Iran and northward to Ghayen. This suture zone separates Lut Block from Afghan Block (Fig. 1a). Rifting between Lut Block and Afghan Block took place in Cretaceous [6]. This suture zone is younger than Neo-Tethys, a deformed accretionary prism and a flanking forearc basin extending from Birjand southeast to Zahedan. The accretionary prism at 32 degrees N is subdivided into two northwest-trending en echelon belts termed the "Ratuk" and "Neh" complexes, respectively. Extensive post-Miocene right-slip faulting is inferred to be an effect of Miocene "terminal" collision of Arabia and Eurasia [6]. These faults are causing a large scale feather appearance (Fig. 1b). Volcanic and some plutonic rocks of the Lut Block are the result of west dipping subduction zone.

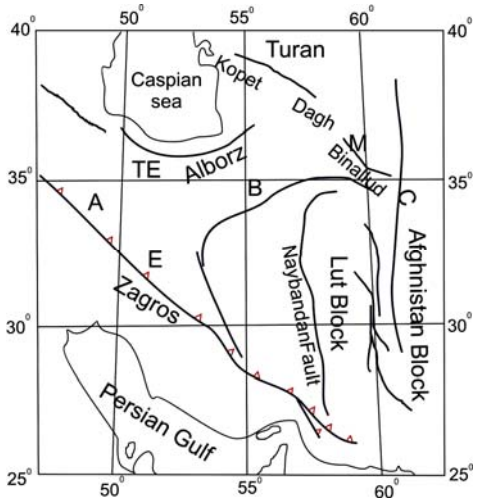

Figure 1a. Schematic structural map of Iran. A: Zagros fracture zone, b: Great Kevir fault, c: Harirud fault, Te: Tehran, M: Mashhad, E: Esfahan [5].

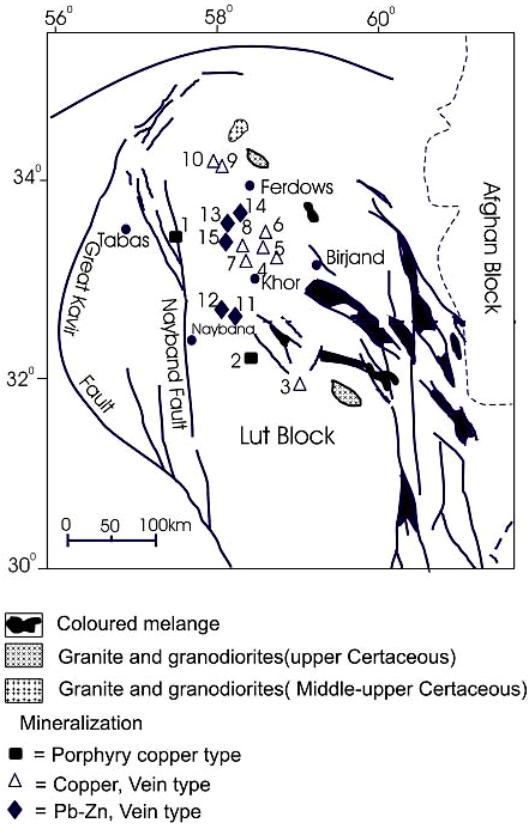

Figure 1b. Map showing Cu, Pb-Zn mineralized area in central lut region. 1-Gazu, 2-Sorkh-Kuh, 3-Qaleh-Zari, 4-Howze Dough, 5-Ghare Kaftar, 6-Shurk, 7-Shikasteh Sabz, 8-Mire Khash, 9-Madan-e-Rahi I, 10-Madan-e-Rahi II, 11-Sehchangi, 12-Howze Rasi, 13-Shurab, 14-Gale Chah, and 15-Chah Nogre [7].

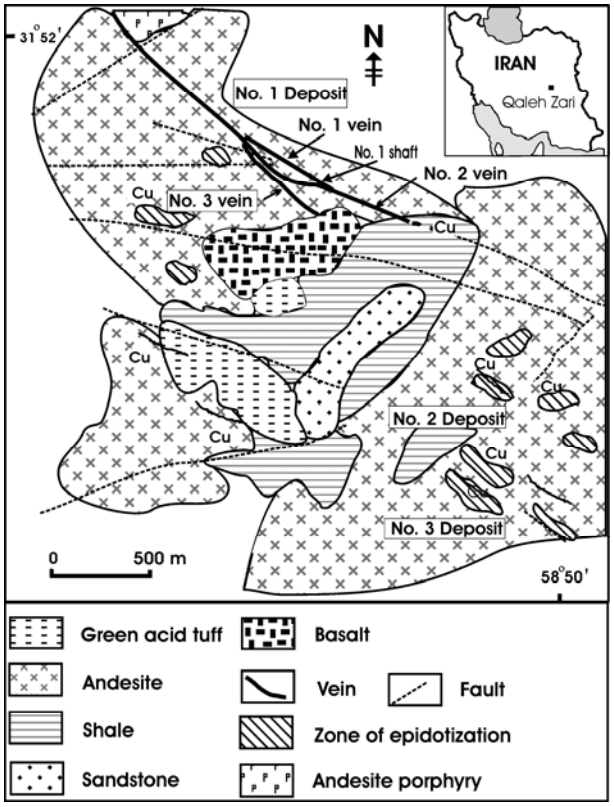

Figure 1c. Geological map of Qaleh-Zari area, revised from [2].

Recent and Quaternary sand dunes, salt flats, and alluvial fans cover large area of Lut Block. The Lut Block is underlain by continental crust of some 40 km thickness [8]. The oldest sediments are from Devonian to Cretaceous. Geological observation and radiometric data indicate that the oldest magmatic activity in the Central Lut took place in the Jurassic time [7]. Rb-Sr isotopic determination of two samples from Shorkh Kuh granite to granodiorites based on whole-rock and biotites of the two samples yield Middle to Late Jurassic age (164.8±1.9 Ma resp. 170±1.9 Ma). In Northern Lut Block, magmatic activity started in the Upper Cretaceous time (75 m.y.) both as volcanic and intrusive rocks.

Maximum volcanic activity took place at the end of Eocene time. The Middle Eocene (47 m.y.) is distinguished by alkaline and shoshonitic volcanism [9]. In addition to calc-alkaline series, basalts and basaltic-andesite were formed in Eocene-Oligocene (40 to 31 m.y.) and Quaternary. The western part of the Central Lut Block is covered by terrestrial volcanic rocks [9]. In Shurab and Khur regions, Kerman Conglomerate occurs as a basis of volcanic sequence dated 39-40 Ma.

Cu and Pb-Zn mineralization related to different episodes of magmatism in Central Lut is shown in Figure 1b. The earliest mineralization is associated with Sorkh-Kuh granite to granodiorites Middle to late Jurassic age (164.8±1.9 Ma resp.170±1.9 Ma). Both disseminated and stockwork mineralization is reported from the contact zone of these intrusive rocks [7]. In Late Cretaceous (75.2±3.5 Ma), porphyry Cu- type mineralization is reported in Gazu area (Fig. 1b) which is associated with intermediate intrusive rocks. Pb-Zn vein types are hosted by volcanic rocks age of 41 to 44 Ma are discovered in Seh Changi, Shurab, and other places (Fig. 1b). Cu-vein-type mineralization is hosted by volcanic rocks age of 39-40 Ma. Qaleh-Zari is the best known (Fig. 1b).

3. Local Geology

The oldest rocks exposed in the mine area are Jurassic shale and sandstone, which form the core of anticline in central part of the Figure 1c. Out side from the mine area, there are some older rock unites presented in Figure 1c. Dome Robah mountain area, Jurassic shale and sandstone are overlapped with angular uncomfortably by a reddish conglomerate of upper Cretaceous age. In upper Cretaceous, a sandy limestone (having 200 m thickness) was deposited on conglomerate. A massive (130 m thickness) pale cream color limestone was deposited, continuous sedimentation in Paleocene time (on the south side of Dome Robah Mountain). Volcanic activity started in this region in Late Eocene time.

Coherent and pyroclastic Tertiary volcanic rocks are dominant in the mine area and in the region. They consist mainly of k-rich andesite and andesitic-basalts, with minor dacite and basalt (Appendix 1). Total Fe of the volcanic rocks in the Qaleh-Zari region is high (TFeO = 6 to 8.4%) mostly presents as Fe_2O_3 (Fe_2O_3 = 2.2 to 5.34 %). Andesitic rocks from the western region of Qaleh-Zari were dated to 40.5 ± 2 Ma [10]. These volcanic rocks are calc-alkaline to K-rich calc-alkaline with transition to shoshonitic association. They have a geochemical signature typical of subduction-related magma [1,11].

Four trends of faults and joints were identified in the mine area (Fig. 1d). From the oldest to youngest they were: 1) a N135°, 75°E trending right lateral strike slip fault with reverse components, 2) N 150°, 80° NE tending set right lateral strike slip fault with reverse components, 3) a NE-SW trending set, and (3) a N 210°, 7o° SE trending right lateral strike slip fault with reverse components and 4) N 120°, 85° NE tending set

left lateral strike slip fault with reverse components (Fig. 1d). The first stage of faulting was brittle and formed a wide zone of breccias. Mineralization is associated within this stage.

All of the Cu and Pb-Zn (vein type) deposits in the Central Lut Block were mainly bounded to the NW-SE faults and fractures system. The NW-SE fracturing system is the extension of the faults and fractures system formed the feather-like mélange and flysch complexes on the east (Fig. 1b).

Three mineralized zones are known in the Qaleh-Zari area. From NW to SE these zones are numbered No. 1 through No. 3 deposits (Fig. 1c). Three major veins are identified in the No. 1 deposit.

4. Sampling and Method of Study

Qaleh-Zari is specularite-rich Cu-Ag-Au deposit. These types of deposits are very rare. This study was taken to find out the genesis of ore bearing fluid.

This study focused on the No. 1 deposit because of underground access. More than 300 ore Samples were collected for petrography, fluid inclusion, electron microprobe, and isotopic analyses. Samples were taken from three veins. At each mine level (70, 100, 135, 170), samples were taken at regular interval (10 m) horizontally. At each locality, samples were collected from the major vein and also small veinlets. The No. 1 shaft (Fig. 1c) was chosen as zero base line for sampling. Samples taken in SE directions were given the prefix of R and those in NW were given a prefix of L.

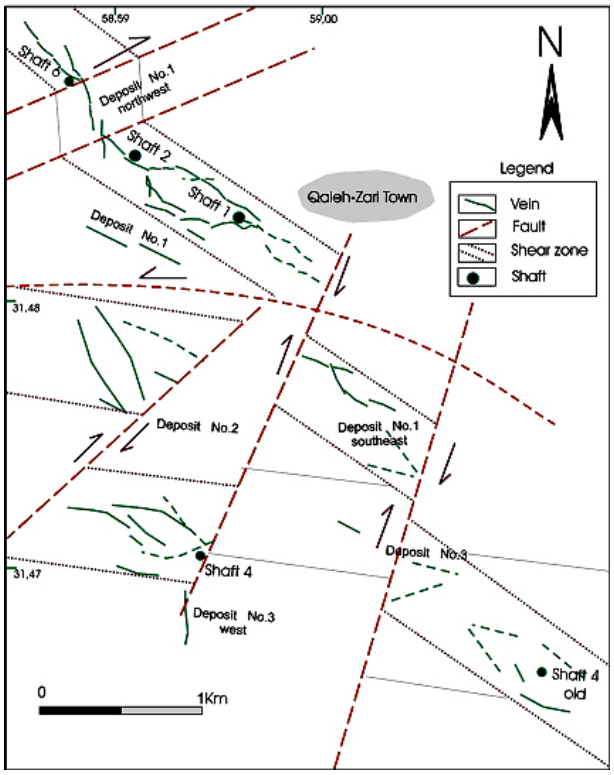

Figure 1d. Tectonic map of Qaleh-Zari mine area.

CAMECA SX50 electron microprobe microanalyser with automated wavelength-dispersive and energy-dispersive analytical systems at the Central Science Laboratory (CSL), University of Tasmania was used. An accelerating voltage of 15 or 20 kV and a stable beam current of 20 or 30 nA were used for the analysis of the chlorites and sulfides. The Proton-Induced X-Ray Emission (PIXE) study was undertaken at the CSIRO Exploration and Mining, Sydney, Australia to analyze the trace element compositions of sulphide minerals.

A Fluid Inc. modified USGS heating/freezing stage was used for fluid inclusion study. The general method and procedure for heating/freezing experiments are reported elsewhere (*e.g.*, Roedder, 1984). The precision of the temperature measurements was less than ±1°C for heating and ±0.3°C for freezing. Accuracy of the measurements was insured by calibration against the triple point of CO2 (−56.6°C), the freezing point of water (0.0°C), the critical point of water (374.6°C) and synthetic fluid inclusions.

Laser Raman spectroscopy (LRS) method is an important development in the field of non-destructive fluid inclusion technique for *in situ* pin-point analysis of individual, unopened fluid inclusions (Roedder, 1984). Laser Raman spectroscopy can be used to quantitatively determine the gaseous components (*e.g.* H2S, CO, CO2, CH4, SO2, H2, NH3, N2) with a detection limit of 0.1 mole% for some species and for identifying daughter minerals. In this study, a DILOR MICRODIL-28® Raman microprobe at the Australian Geological Survey Organisation (AGSO), Canberra was used to quantitatively determine the composition of gaseous components and to identify the daughter minerals in fluid inclusions from the deposit.

5. Mineralization

Mineralized Veins strike N 20° to N 50° W and dip 70° to 90° NE (Fig. 1c). The entire length of mineralized zone is more than 4 Km. Mining activity is mainly focused on the No. 1 deposit, where three major sub-parallel quartz veins are present. No. 2 vein is the main vein and can be traced for more than 3.5 km along strike (N40° W) and more than 350 m down dip (75° to 90° NE) (Fig. 1c). No. 1 vein is about 650 m long and No. 3 is less than 500 m long. Veins are in general very steep and dipping 70° to 90° NE. In the No. 1 and 3

deposits, volcanic rocks host the veins where in No. 2 Jurassic shale and sandstone (Fig. 1c) host the deposit. Textures, such as crustification, comb structures, symmetrical banding, cockade structure and cavities, which are indicative of open space filling, are present.

Paragenesis

In all veins quartz is by far the most common constituent. Coarse-grained bands of euhedral dogtooth clear quartz occurs in all places. The larger clear euhedral quartz crystals terminate within open cavities. Hematite (specularite) is the most abundant oxide after quartz (up to 25%). Mineralization can be divided into 4 stages based on crosscutting relation and temperatures of homogenization of fluid inclusions (see later section) (Fig. 2).

Stage I: The earliest paragenetic stage is characterized by hematite (specularite), chlorite, quartz, chalcopyrite, and Cu-Pb-Bi-Ag sulfosalt minerals (*e.g.* aikinite, a proton microprobe mineral). Deposited Sulfosalts on this stage are: aikinite, matildite, Bi-rich galena, and wittichinite. Most of sulfosalts are found as inclusion within chalcopyrite. Quartz veins and veinlets typically have hematite bands in the margins. Quartz formed as 1-10 cm clear crystals. Silver is present as sulfosalt minerals that are mainly found as inclusion within chalcopyrite. Chlorites were formed either due to alteration of hornblende, biotite, and pyroxene within the country rocks as part of propylitic assemblages, or they crystallized directly from the hydrothermal fluid into the veins. Chlorites, directly crystallized from the hydrothermal fluid, are situated mainly in the vein. Hematite (specularite) forms 10 to 25 percent of the veins. Most of chalcopyrite, sulfosalts, and hematite were deposited in this stage. In all veins (along the veins and down deep) hematite formed first, followed by the clear quartz-chlorite and then by chalcopyrite and occasionally pyrite (Fig. 3a-b). Electrum was identified in only one, out of 200 polished section examined.

Stage II: quartz, chalcopyrite, pyrite, chlorite ± hematite ± sulfosalt minerals. This stage is less important in comparison with the first stage. Pyrite forms mainly euhedral crystals and is more abundant in this stage. Sulfosalts formed at this stage are: arcubisite, wittichinite, aikinite, cosalite-berryite, Ag-rich sulfosalts, and Ag-rich galena. Quartz are very clear and formed very large crystals (up to 20 cm long).

Stage III: quartz ± pyrite ± chalcopyrite. This stage is present only as small veinlets. Quartz crystals are becoming less clear. Very minor chalcopyrite is associated with these veins.

Stage IV: hematite + quartz + calcite ± pyrite ± chalcopyrite ± Ag-rich sulfosalts. Calcites are clear to milky. They are grown over the quartz crystals or they form crystals of different shape. Similar to stage I, hematite formed first followed by quartz. Occasionally pyrite and chalcopyrite are found on this stage. Calcite is abundant in the No. 3 deposit.

6. Alteration

Propylitic alteration assemblages are very widespread in the Qaleh-Zari area (Fig. 1c). Epidote and chlorite are the two characteristic minerals of this assemblage. Epidote is very abundant and formed by alteration of plagioclase, pyroxene, and hornblende. Epidote is also abundant as veinlets filling the joints. Chlorite formed by alteration of mafic minerals or directly from the ore fluid within the vein. Chlorites are generally Fe-rich types such as ripidolite with minor bronsvigite-pycnochlorite [12]. Argillic alteration is locally present (Fig. 1c). Silicification is mainly found within a zone adjacent to the veins.

7. Ore Grade Distribution

Table 1 summarizes the typical ore grades and width of veins. To determine the distribution of and correlation between Cu, Ag and Au, mine assay data were used to contour grade variations along long sections of the No. 1 (Figs. 4-6) and 3 veins (Figs. 7-9). Ore grades are presented on cross sections.

In the No. 1 vein there are two zones with higher Cu-contents (Fig. 4). In zone A, the highest Cu ore grade (Cu=7%) was occurs mainly in area between 100 to 135 m mine level. In zone B, the highest Cu ore grade (Cu = 6 %) occurs mainly in an area between 70 to 170 m mine levels (Fig. 4). In zone A, the Cu-ore grade decreases toward the surface in NW direction (Fig. 4). The highest Ag contents (160 to 180 ppm) is coincident with the high grade copper ore body (Fig. 5). The highest Au contents (to 4.5 ppm) are situated between 70 to 100 meter mine levels (Fig. 6). In zone B, the high Au grades (2 ppm) are mainly associated with high Cu grades (Fig. 6).

In the No. 3 vein the highest Cu (to 8.5%) and Ag (325-400 ppm) grades occur mainly between the 100 and 135 m mine levels (Fig. 7). The close association of Ag-bearing sulfosalts with chalcopyrite accounts for this close Cu-Ag association. This explains the association and distribution of high grade Cu and Ag of the ore. The highest Au (Au = 30-40 ppm) is found in No. 3 vein. It occurs in area between 40 to 100 meters mine levels (Fig. 9).

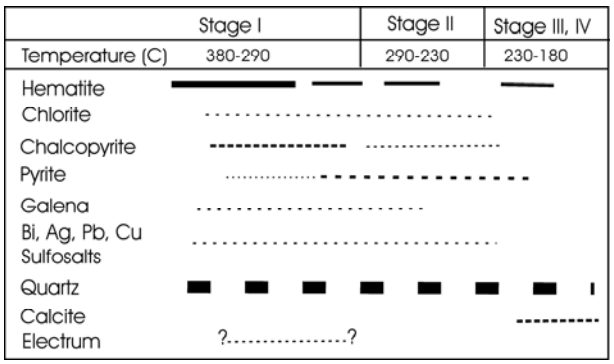

Figure 2. Mineral paragenesis of Qaleh-Zari Cu-Au-Ag deposit.

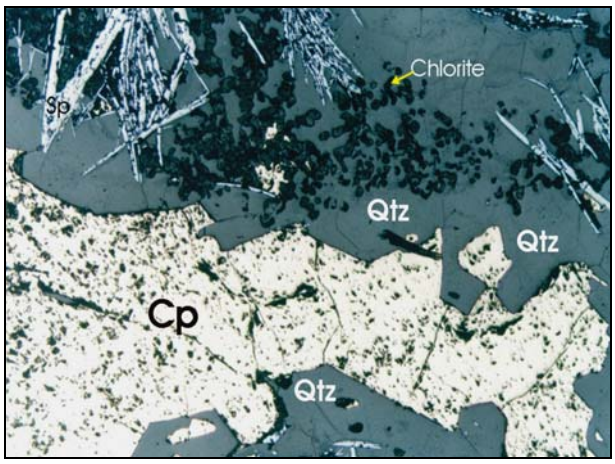

Figure 3a. Photomicrograph shows the sequence of mineralization, specularite (sp) and chlorite crystallized first, then quartz (Qtz) and finally chalcopyrite (Cp).

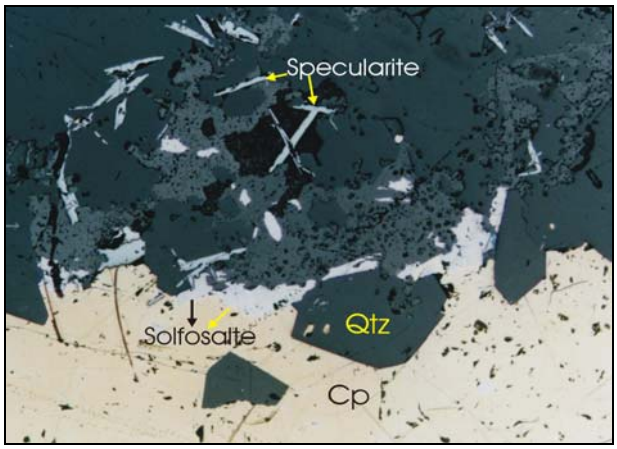

Figure 3b. Photomicrograph shows specularite formed first, quartz with euhedral shape fallow the specularite, chalcopyrite and sulfosalts are formed later.

Table 1. The average ore grade and width of veins [2]

Vein	1	2	2	3
%Cu	7	8.7	8.9	7.3
Au (ppm)	4.5	0.3	8.7	40
Ag (ppm)	180	246	620	255
%Bi	n.a	n.a	0.28	0.24
%Pb	n.a	n.a	0.33	0.13
%Zn	n.a	n.a	0.1	0.03
%As	n.a	n.a	0.007	0.005
%Fe	n.a	n.a	27.6	24
%SiO2	n.a	n.a	29.2	36.6
%Ca	n.a	n.a	2	1.5

n.a not available

8. Fluid Inclusion Studies

Fluid inclusion studies were carried out on 27 doubly polished plates chosen from three veins at different depth. Quartz from all paragenetic stages was studied, based on the paragenesis of hypogene minerals and late secondary mineralization based on crosscutting relation and textural study. Primary fluid inclusions in all quartz veins are simple two phase liquid-vapor inclusions (Fig. 10). These inclusions contain liquid and vapor with minor CO_2 and no daughter minerals. The vapor bubble makes up 10 to 32 percent of the inclusion volume. These inclusions measured 3 to 27 μm in diameter.

Homogenization of Temperatures and Salinities

Heating and freezing measurement were carried out on a U.S. Geological Survey heating freezing stage with precision of ± 2°C. Homogenization measurements were carried out first to avoid stretching of inclusions. No clathrate formation was observed in any of the fluid inclusions during freezing. The absence of clathrates indicates that the CO_2 content of fluid was less than 2 wt percent [12]. Laser Raman analysis of fluid inclusions also detected minor (1-2 mole%) CO_2. Salinities were calculated using the equation of Bozzo *et al.* [14].

Stage I quartz: Temperatures of homogenization of primary fluid inclusions from Stage I quartz ranged from 260° to 400° C (Fig. 11; Appendix 2). Salinities ranged from 2 to 5.5 wt % NaCl equiv (Appendix 2). In the No. 1 vein, the Th: one with Th distribution is bimodal, with one mode at 370°C and the second mode at 315°C. The highest temperatures of homogenization are around No. 1 shaft and it decreases to the NW.

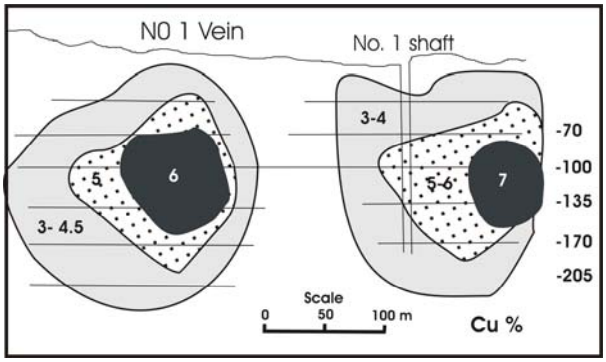

Figure 4. Cross section showing distribution of Cu grade in vein No. 1.

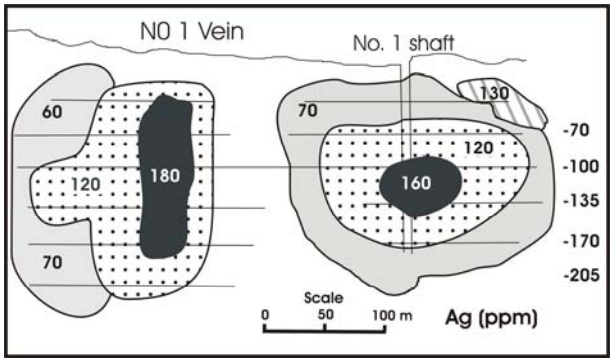

Figure 5. Cross section showing distribution of Ag grade in vein No. 1.

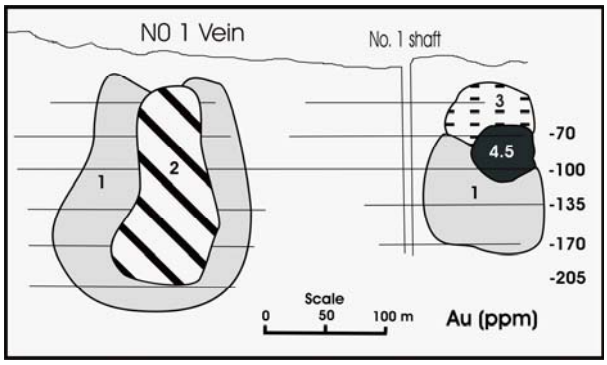

Figure 6. Cross section showing distribution of Au grade in vein No. 1.

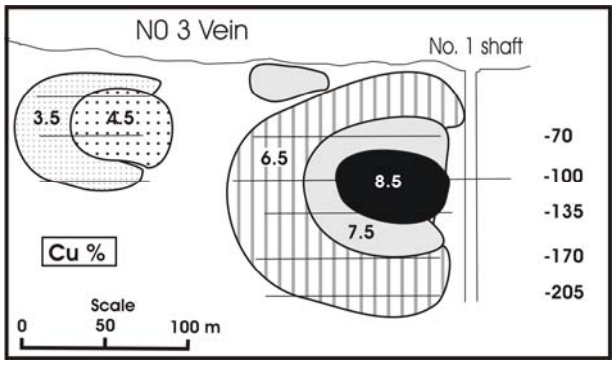

Figure 7. Cross section showing distribution of Cu grade in vein No. 3.

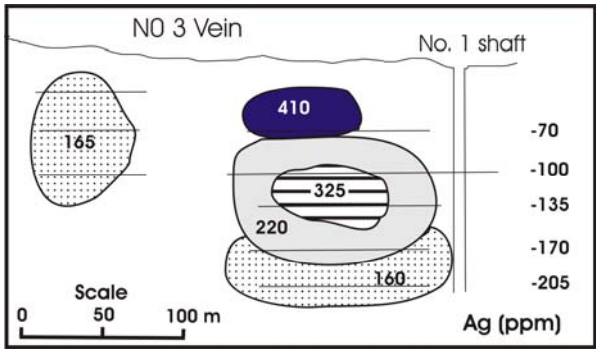

Figure 8. Cross section showing distribution of Ag grade in vein No. 3.

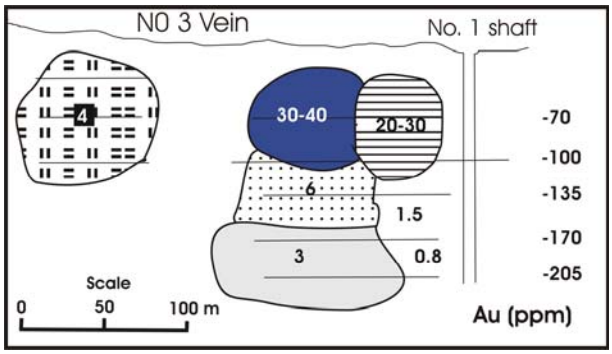

Figure 9. Cross section showing distribution of Au grade in vein No. 3.

In the No. 2 vein, Th are between 295° to 370°C, with a mode at 325°-350°C (Fig. 11; Appendix 2). In the No. 3 vein, the mode of Th is between 300° and 310°C (Fig. 11; Appendix 1). Although temperatures of homogenization for Stage I quartz are similar in the No. 1 & 2 veins, Th in the No. 3 vein is significantly lower.

Stage II quartz: Temperatures of homogenization of primary fluid inclusions from Stage II quartz ranged from 230° to 290°C (Fig. 11; Appendix 3). Salinities ranged from 2.2 to 5.8 wt % NaCl equiv (Appendix 3).

Stage III quartz: Temperatures of homogenization of primary fluid inclusions from Stage III quartz ranged

from 240° to 256°C (Fig. 11; Appendix 4) Salinities ranged from 1.8 to 2.3 wt % NaCl equiv (Appendix 4).

Stage IV quartz: Temperatures of homogenization of primary fluid inclusions from this Stage IV quartz ranged from 180° to 210°C (Fig. 11; Appendix 4). Salinities of these inclusions ranged from 1.3 to 1.8 wt % NaCl equiv (Appendix 4).

Discussion: The salinity of the ore fluid appears to have decreased from about 6 wt % NaCl equiv in the earliest stage of mineralization to 1 wt % NaCl in latest stage of mineralization (Fig. 12). Most of the chalcopyrite and sulfosalts minerals were deposited early in the paragenesis at high temperatures commonly in excess of 300°C, mainly hematite, quartz, and calcite were deposited.

Laser Raman analysis of fluid inclusions detected minor (to 1-2 mole%) CO_2 in the vapor phase, but no methane and N_2 in the vapor phase, nor any sulfate in the liquid.

9. Carbon Oxygen Isotopes

Calcite samples, which formed during the hypogene stage of mineralization, were analyzed for C and O isotopes at the University of Tasmania (Table 2). Based on temperature of fluid inclusions in quartz crystals, calcite formed at 200-250°C using a temperature of 200°C and fractionation data of O'Neil *et al.* [15] and Ohmoto and Rye [16], the fluid $\delta^{18}O_{SMOW}$ was estimated at 7.4 to 9.8‰, and CO_2 in the fluid had $\delta^{13}C_{PDB}$ of −3.8 to −3.0‰. When compared to other Cu deposits, Qaleh Zari carbonates had similar isotopic composition to those from porphyry Cu deposits (Fig. 13). The fluid $\delta^{18}O_{SMOW}$ overlaps the range of magmatic waters, but is inconsistent with that of meteoric waters [17]. The $\delta^{18}O$ of quartz studied by Hassan Nejad [18] also indicates a magmatic source for the water.

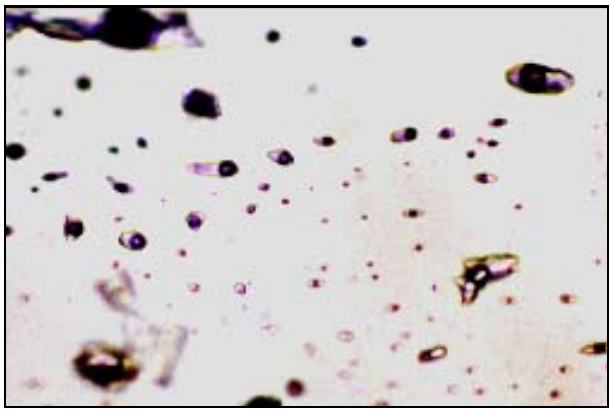

Figure 10. Photomicrograph showing the fluid inclusion in quartz, from Qaleh-Zari Mine. They are liquid rich type.

10. Sulfur Isotopes

Eight chalcopyrite and two pyrite were selected from different veins which are formed within the first and second stage of mineralization (Table 3). Chalcopyrite and pyrite were extracted using a drill from different veins and analyzed for $\delta^{34}S_{CDT}$ at the University of Tasmania, where sample reproducibility is typically ±0.2‰. The results are summarized in Table 3 and plotted in Figure 14. $\delta^{34}S_{CDT}$ values of chalcopyrite separates vary between 0.4 and 2.2‰, and for pyrite separates vary between 2.0 and 2.2‰. Using fractionation equations in Ohmoto and Rye [16] and a temperature estimate of 250-300°C, the $\delta^{34}S_{CDT}$ of the fluid was between 0.5 to 1.9‰. The sulfur may be originated from the following sources: 1) direct input from buried magmatic pluton, 2) leached from host volcanic rocks, or 3) leached from the nearby sedimentary rocks. Jurassic shale in the area is carbonaceous and it is found only in the middle part of the area. The Qaleh-Zari ore bearing fluid was very oxidizing (because of at least 20% specularite) and it did not appear to interact with the Jurassic carbonaceous shale, therefore sulfur is not likely originated from the shale.

11. Chlorite Geochemistry

Chlorites were formed either due to alteration of hornblende, biotite, and pyroxene within the country rocks as part of propylitic assemblages, or they crystallized directly from the hydrothermal fluid into the veins (Fig. 15). Chlorites crystallized directly from the hydrothermal fluid are situated mainly in the vein. To compare the temperature of fluid inclusion with chlorite and also determining the physiochemical condition of ore bearing fluid chlorite from different veins and from different stages of mineralization were analyzed. Following detailed petrography studies, chlorites next to quartz were selected (within the vein zone) for Cameca SX 50 electron microprobe EDS analysis at the University of Tasmania. An accelerating voltage of 15 kV was used with a beam current of 20 nA. Chlorites are generally, Fe-rich types such as ripidolite with minor bronsvigite-pycnochlorite (Fig. 16).

Using the equation of Cathelineau, the temperature of chlorite formation was calculated. The temperature of fluid inclusion in quartz and chlorite formed next to each other for 17 samples from three different veins were then compared. In all cases, the calculated temperature of chlorite was 15° to 20°C less than the homogenization temperature of fluid inclusions.

Noting this systematic difference and that the Cathelineau and Nieva [19] equation was extrapolation

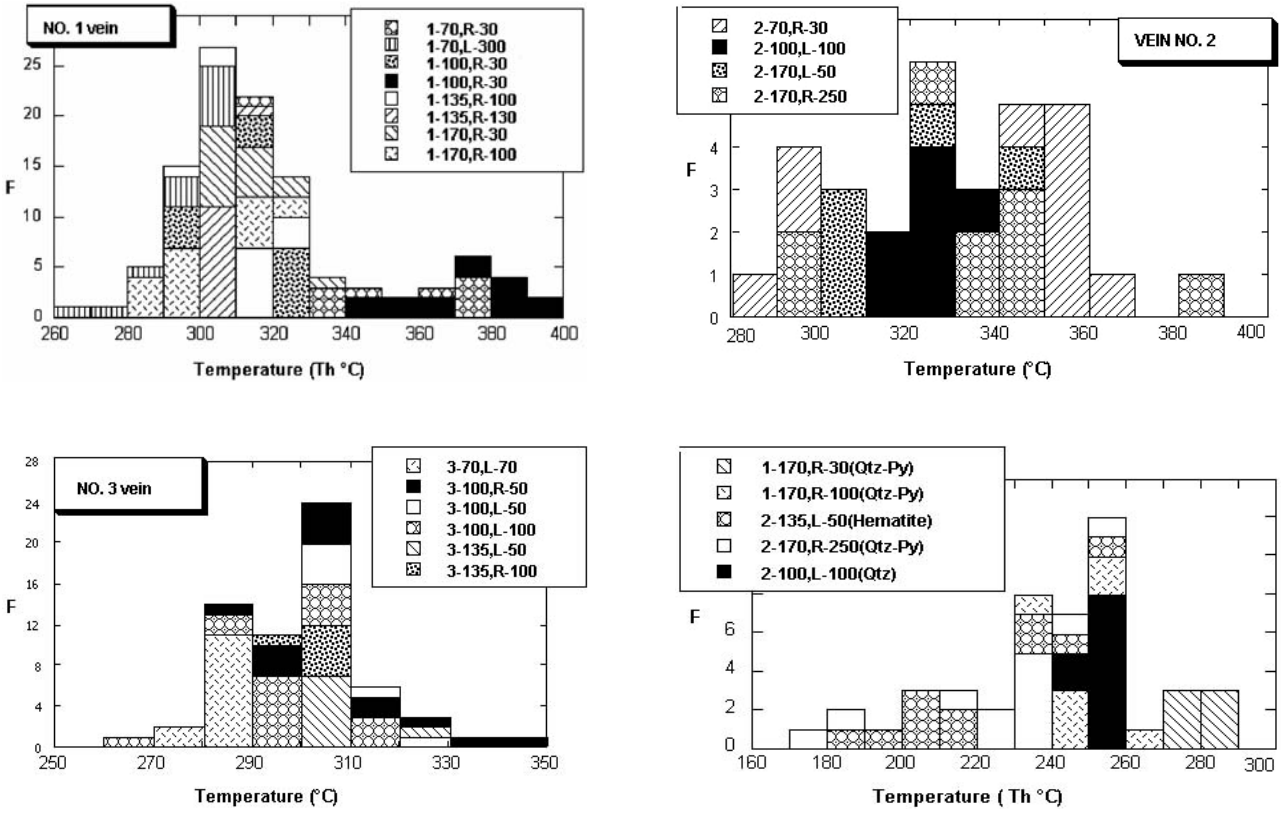

Figure 11. Histogram of the distribution of liquid-vapor homogenization temperature (Th) of fluid inclusions in quartz from selected samples in different levels of No. 1, 2, 3 vein. (Th) of fluid inclusions in quartz from stage II (1-170, R-30), 1-170, R-100, 2-170, R-250), stage III (2-100, L-100), and stage IV (2-135, L-500). Sample location (meter) from shaft No.1 (R) to the right and (L) to the left. Mine level (70, 100, 135, 170).

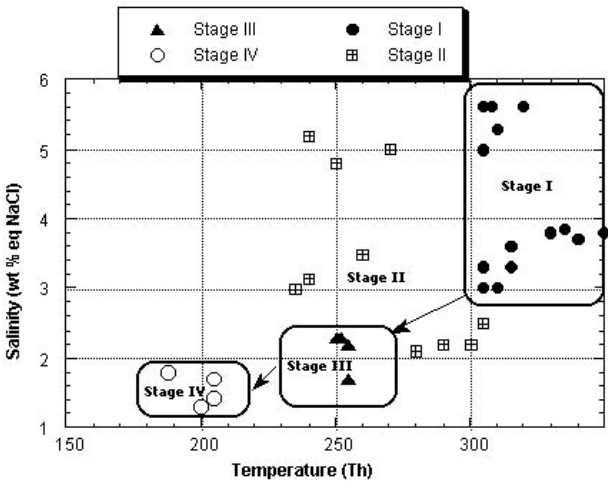

Figure 12. Plot of salinity *vs.* temperature (Th) for different stage of mineralization. In general, inclusions formed in early stage have higher salinity (3-6% eq NaCl) than those formed later.

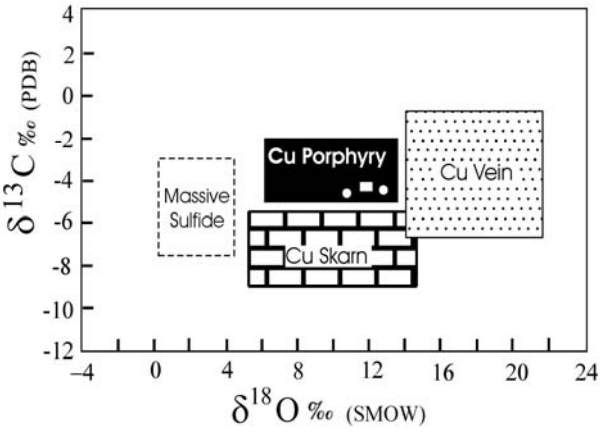

Figure 13. Oxygen and carbon isotopic composition of calcite formed in late stage of mineralization at Qaleh- Zari compared with different types of Cu deposits. Oxygen and carbon isotopic composition of Qaleh-Zari fall in the field of porphyry copper deposit.

Table 2. Carbon and Oxygen isotopic composition of Calcite and fluid at T 200°C

Sample No.	$\delta^{18}O_{SMOW}$ (‰)		$\delta^{13}C_{PDB}$ (‰)	
	Calcite	Fluid	Calcite	CO_2
Vein-1 (3972)	17.41	7.86	−3.36	−3.54
Vein-1 (3973)	19.40	9.8	−2.86	−3.04
Vein-2 (3974)	16.96	7.47	−3.61	−3.79

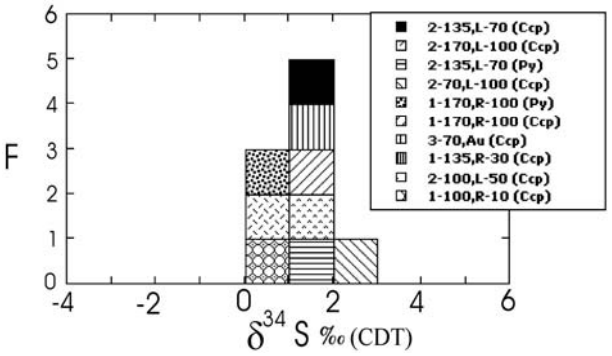

Figure 14. Histogram of S-isotopic composition of pyrite and chalcopyrite from selected samples in different mine levels of No. 1, 2, and 3 veins.

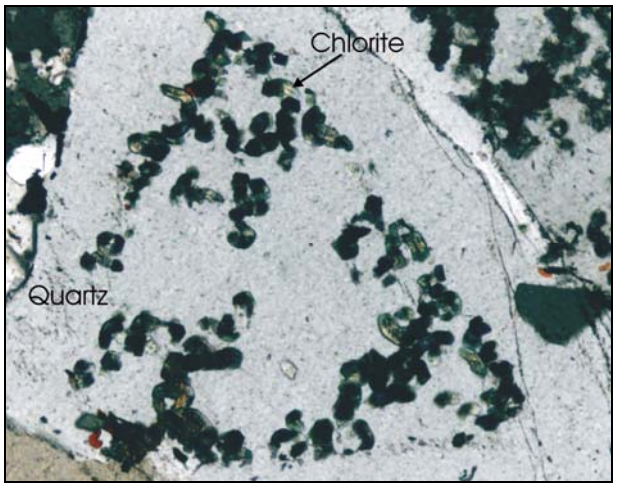

Figure 15. Photomicrograph shows that chlorite formed the same time as quartz crystal was growing.

for temperatures above 240°C, Karimpour and Zaw [12] proposed a new equation for estimating temperatures from chlorite composition:0.0039T = Al^{IV} - 0.0756, where T is in Kelvin and Al^{IV} is based on 14 oxygen atoms (Fig. 17).

By using Walshe & Solomon [20] and Walshe [20] procedures, both temperature and logfO_2 formation of chlorite were calculated. Temperature was lower than fluid inclusion. The logfO_2 of formation of chlorite was calculated using Walshe & Solomon [20] and Walshe [21] procedures. The results indicate that chlorite formed in the field of magnetite. More than 250 polished section and thin section were studied from different veins at different depth. No magnetite was found to form from hydrothermal fluid at Qaleh-Zari. Hematite (specularite) is the only primary iron oxides present at Qlaeh-Zari. Therefore based on very detail and accurate fluid inclusion thermometry and paragenesis study, both Walshe & Solomon [20] and Walshe [21] and Cathelineau and Nieva [19] methods for calculating the temperature of formation of chlorite and determining the logfO_2 has some problems or chlorite is not a reliable mineral to use for calculating the temperature of formation or determining the logfO_2 of the fluid.

MgO and FeO content of chlorites changed with respect to temperature. The FeO content of chlorite was 37 wt % at 310°C and decreased to about 29 % at 260°C. The MgO content of chlorite increased while the temperature of fluid was decreasing. The MgO content was about 8% at 310°C and increased to 13.5 % at 260°C.

12. Trace Element Contents of Chalcopyrite and Pyrite

As mineragraphic investigations indicated that electrum could not account for the observed Au grades in the Qaleh-Zari deposit, a proton microprobe study using the HIAF Proton Microprobe at CSIRO in Sydney was undertaken to establish the mineralogical host to Au. Table 4 lists analytical results for analysis of pyrite and chalcopyrite and an analysis of aikinite.

Pyrite

Based on trace element content**,** pyrite can be divided into two groups. The first group is characterized by high As (to 2800 ppm) with associated high Au (to 20 ppm), Mo (to 4.3 ppm) and Se (to 190 ppm). In contrast, the second group has much lower As values, but is enriched in Zn (to 200 ppm), Pb (to 190 ppm), Sn (to 17 ppm), Sb (to 6 ppm) and Cd (to 6 ppm) relative to the first group. The Cu content of both groups is similar, with values between 54 to 870 ppm.

The enrichment of Au in As-rich pyrite has been observed in a number of deposit types including, among others, lode Au [22,23] and volcanic-hosted massive

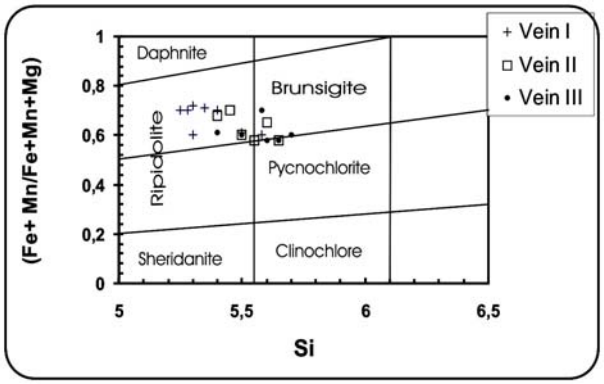

Figure 16. Plot shows types of chlorites formed in No. 1, 2, and 3 veins.

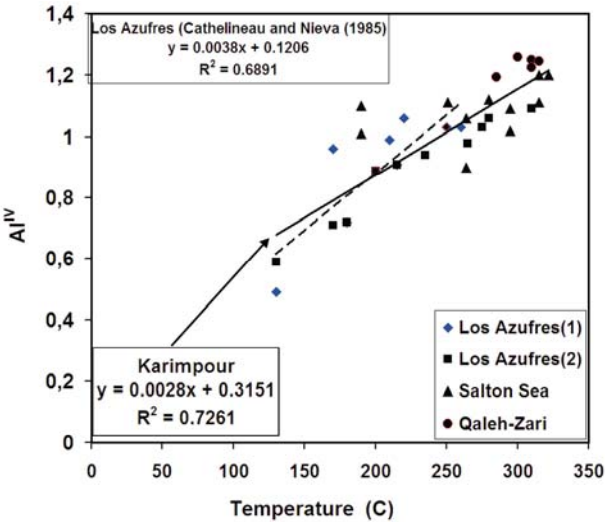

Figure 17. Equation of Cathelineau and Nieva (1985) and Karimpour.

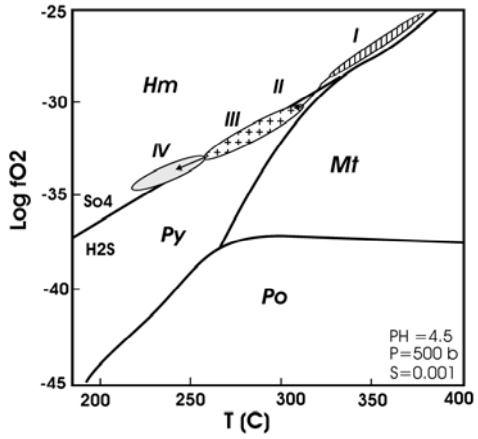

Figure 18. Plot of Log fO_2 – T, at pH= 4.5, $m\sum S\ 10^{-3}$, P= 500 b. At Qaleh-Zari due to high oxygen fugacity and low sulfur specularite was formed first and pyrite formed only within the 2nd and 3rd stage of mineralization. At the last stage (IV), specularite was dominant.

sulfide deposits [24,25]. Although a great amount of uncertainty exist regarding the causes of this association, recent work by Simon *et al.* [26,27] indicate that gold bearing from the Twin Creek Carlin-type gold deposits show that gold is present as both Au^0 and Au^{1+} and arsenic present as As^{1-}. Au^0 is present as sub-micrometer size inclusions of free gold, whereas Au^{1+} is attributed to gold in the lattice of arsenian pyrite.

The generally high Se levels in the pyrite (and in the chalcopyrite; see below) indicate deposition from either an oxidized fluid or a fluid with a high Se/S ratio [28]. Such fluid is consistent with derivation from a magmatic-hydrothermal source

Chalcopyrite

Chalcopyrite was also divided into two groups based on paragenesis. The first group is characterized by high Ag (to 44 ppm) and Ba (to 360 ppm), whereas the second group is characterized by high Zn (to 470 ppm). Both groups lack detectable As, Te, Tl, Mo, Co, and Ni, but contain significant Se (to 110 ppm), Sn (to 42 ppm), Cd (to 33 ppm) and Au (to 42 ppm). These data confirm the Se-rich character of Qaleh-Zari sulfides and suggest that chalcopyrite may be a significant repository of Au. Experiments in the Au-Cu-Fe-S system were carried out at 400°C to 700°C to determine how much gold could be accommodated by bornite and chalcopyrite [29]. Results show that for all temperatures bornite contains one order of magnitude more gold than chalcopyrite. The range of gold concentrations in bornite and chalcopyrite decreases with decreasing temperature [29].

Sulfosalt Minerals

A single analysis of aikinite ($CuPbBiS_3$) suggests enrichment in Te (756 ppm), Re (332 ppm), Se (0.179 %), and Sb (34.8 ppm; Table 5) in addition to Ag (0.45%). This analysis suggests that sulfosalt minerals are probably the most significant repositories of Ag.

13. Ore Transport and Deposition

Based on our fluid inclusion data, the Qaleh-Zari ore fluids decreased from temperatures in excess of 350°C in Stage I to less than 200°C in stage IV. There was a corresponding decrease in salinities from 5-6 to ~2 eq wt % NaCl. Variations in homogenization temperatures of stage I fluid inclusions relative to shaft 1 suggest that this variation was spatial as well as temporal. These data suggest either the ore fluid evolved in time and space or that a high temperature and salinity fluid mixed with a lower temperature and salinity fluid at Qaleh-Zari.

Table 3. Sulfur isotopic composition of pyrite and chalcopyrite and fluid (T 300°C for chalcopyrite and 250°C for pyrite) Sample location (meter) from shaft No.1 (R) to the right and (L) to the left

Vein	Depth	Based on shaft No.1	Mineral	$\delta^{34}S$ of Mineral	$\delta^{34}S$ in H_2S
1	100	R-10	Chalcopyrite	0.4	0.552
1	135	R-30	Chalcopyrite	1.4	1.55
1	170	R-100	Chalcopyrite	1.8	1.92
1	170	R-100	Pyrite	2.0	0.54
2	70	L-100	Chalcopyrite	2.2	2.35
2	100	L-70	Chalcopyrite	1.8	1.92
2	135	L-70	Chalcopyrite	1.5	1.65
2	135	L-70	pyrite	2.2	0.74
2	170	L-100	Chalcopyrite	0.6	0.75
3	70	Au	Chalcopyrite	1.3	1.45

Table 4. Trace elemental content of pyrite, chalcopyrite, and sulfosalt (in ppm or %)

Element	Chalcopyrite		Pyrite		Sulfosalt Cu-Ag-Bi-Pb
	Grope A Range	Grope B Range	Grope A Range	Grope B Range	
Cu	34.5 %	34.5-34.6 %	54-871	255-292	2.817 %
As	n.d	n.d	2200-2800	31-474	n.d
Zn	125-318	312-470	15-24	4-202	n.d
Pb	29-50	3-60	4-63	87-186	6.53 %
Bi	20-24	8-19	1.5-885	24-63	6.77 %
Sn	42	15-40	0-13	12-17	n.d
Au	0-42	3-30	6.5-19.3	0-12	n.d
Ag	26-44	11	0-270	14	0.446 %
Mo	n.d	n.d	1.7-4.3	n.d	n.d
Sb	1.6-26	0-16	0-2.3	4-6	34.8
Te	n.d	n.d	10-20	18	756
Tl	n.d	n.d	n.d	n.d	576
Se	110	66-80	189	89	1790
Co	n.d	n.d	102-233	100-298	n.a
Ni	n.d	n.d	n.d	0-10	n.a
Cd	13-33	19-24	0-1.7	4-6.3	n.a
Ba	201-363	140-163	89	52-85	n.a
Sr	176-212	106-220	30-35	40-55	n.a
Zr	85	44-74	10-13	14-22	n.a
Y	n.d	n.d	0.5	5	n.a
In	5-36	0-1	8.5-10	13	6.4
Re	n.a	n.a	n.a	n.a	332

n.d = not detected, n.a = not analyzed

Hematite, the predominant Fe-S-O mineral in the Qaleh-Zari vein is stable at all temperatures at highly oxidized conditions (*i.e.* $*SO_4 > *H_2S$), but it is also stable at high temperature in moderately oxidized conditions (*i.e.* $*H_2S * *SO_4$) if *S is low (Fig. 18). Although the presence of hematite in the ore stages indicates relatively low H_2S, the redox conditions (*i.e.* $*SO_4 > *H_2S$ verses $*H_2S * *SO_4$) cannot be determined by the Fe-O-S mineral assemblages.

However, the sulfur isotope data suggest that the conditions were H_2S dominant (*i.e.* moderately oxidized with $*H_2S * *SO_4$). The range in δ34S or sulfide minerals reported in this study is narrow (0.4-2.2), which is inconsistent with highly oxidized conditions ($*SO_4 > *H_2S$) where a much larger range in d34S would be expected [30]. Using these isotopic constraints and the mineralogical and fluid inclusion data, the fluid conditions inferred for paragenetic stages I to IV are plotted on Figure 18. Although the fluids decreased in temperature and salinity temporally and spatially, no major changes in redox relative to $*H_2S/*SO_4$ were necessary. Such trajectory in fO_2-temperature space could be produced either by rock buffered cooling or by mixing of a high temperature ore fluid (possibly magmatic) with a lower temperature ambient (possibly meteoric) fluid. As the salinity also varies between paragenetic stages, we prefer the fluid mixing model. This simple mixing model can easily account for the deposition of Cu, Au and Ag in the veins. Figure 20 illustrates that the solubility of Cu as a chloride complex decreases rapidly with temperature, with the stage III fluids only capable of carrying minor Cu. The mechanism of Au transport and deposition is more problematic. For the conditions inferred for stage I ore fluids (*e.g.* 300-400°C, 5.5 wt % NaCl, 10^{-3} *m* H_2S, pH of 4.5), gold could have been carried either by chlorocomplexes or thiocomplexes, depending on the exact sulfur content and pH of the ore fluids (*c.f.* Huston, 2000). In either case, however, fluid mixing would have effectively deposited gold, either by dilution (reducing $*H_2S$ in the case of gold thiocomplexes or reducing salinity for gold chlorocomplexes) or by cooling (for gold chlorocomplexes). Hence, the depositional mechanism at Qaleh-Zari is most likely simple fluid mixing, and it does not appear to involve redox reactions as at some other Fe-oxide-related Cu-Au deposits.

14. Conclusion

Tertiary volcanic rocks cover an area more than 400 km^2. The Qaleh-Zari Cu-Ag-Au mineralization is localized and is present in small region of the volcanic rocks. The Qaleh-Zari deposit consists of a series of specularite-rich Cu-Au-Ag-bearing vein deposits. Host rocks are mainly Tertiary andesite and andesitic basalts, but in the central part shale and sandstone of Jurassic age. Andesitic rocks from the western region of Qaleh-Zari were dated to 40.5 ± 2 Ma [10]. These volcanic rocks are calc-alkaline to K-rich calc-alkaline with transition to shoshonitic association. They have a geochemical signature typical of subduction-related magma [1,11].

The Qaleh-Zari Cu-Ag-Au deposit has several unique and important features such as: 1) high grade Cu-Ag-Au deposit. 2) the ore fluid is very oxidizing as evidenced by the presence of abundant specularite, 3) no magnetite is formed from the ore fluid, 4) low sulfide, 5) moderate to high temperature with moderate to low salinities.

Most of chalcopyrite and some sulfosalt minerals were deposited at temperature of 350° to 290°C. The oxygen isotopic values (measured from calcite) indicate that the fluid had a magmatic origin. Both C and S isotopic values also suggest magmatic affinities. It is interpreted that an intermediate subvolcanic stock at depth was the source of ore fluid. The moderate to low salinities of ore fluids indicate that input of meteoric fluids during the later stages of mineralization cannot be ruled out. The style of mineralization may change with depth to porphyry type. Shape and depth of porphyry style of mineralization can be defined using appropriate geophysical method.

Acknowledgements

We would like to thank to Iranian industrial Copper company and Minakan Mining company for allowing access to Qaleh-Zari mine and also to geologist working at Qaleh-Zari mine for being very cooperative. The authors wish to thank Dr Ross R Large director of Centre for Ore Deposit Research, University of Tasmania, Hobart, Australia for accessing the research facilities. Thanks to people working in Central Sciences Laboratory, University of Tasmania for electron microprobe analysis and S, C, and O isotopes determination.

References

1. Sadaghyani-Avval F., Etude geologique de la region de la mine de Khali-Eh-Zari (Iran) mineralization et inclusions fluids. Ph.D. *Theses*, unpublished equipe de recherche aur les equilibrites entre fluides et mineraux, Universite de Nancy I., 165 p. (1976).
2. Yuichi S., Ogawa K., and Akiyama N. Copper ores from Qaleh Zari mine, Iran. *Mining Geology*, **26**: 385-391 (1976).

3. DaymehVar M. Geology and geochemistry of Qaleh-Zari Cu-Au deposit: Unpublished, M.Sc. *Thesis*, University of Tarbite Modaress, Iran (1993).
4. Hassan Nejad A.A. Geology and Geochemistry of Qaleh-Zari Cu-Au-Ag deposit. Unpublished, M.Sc. *Thesis*, University of Shiraz, Iran (1993).
5. Soffel H.C. and Forster H.G. Polar Wander path of Central-East-Iran microplate including new results. *N. Jb. Geol. Palaont. Abh.*, **168**(2/3): 165-172 (1984).
6. Tirrul R., Bell L.R., Griffis R.J., and Camp V.E. The Sistan suture zone of eastern Iran. *G.S.A. Bulletin*, **84**: 134-150 (1983).
7. Tarkian M., Lotfi M., and Baumann A. Magmatic copper and Lead Zinc ore deposits in the Central Lut, Eastern Iran. *N. Jb. Geol. Palaont. Abh*., **168**(2/3): 497-523 (1984).
8. Dehghani G. Schwerefeld und Krustenaufbau im Iran-Humburger Geophys. Einzelscher., R. A., H., 54, S., Hamburg (1981).
9. Lensch G. and Schmidt K. Plate tectonic, orogeny, and mineralization in the Iranian fold belts results and conclusions. *N. Jb. Geol. Palaont. Abh.*, **168**(2/3): 558-568 (1984).
10. Kluyver H.M., Griffts R.J., Tirrul R., Chance P.N., and Meixner H.M. Geological Quadrangle Map Sheet Lakar Kuh Quadrangle 1:250,000. Geol. Surv. Iran (1978).
11. Tarkian M., Lotfi M. and Bauman A. Tectonic, magmatism and the formation of mineral deposits in central Lut, East of Iran. Geol. Survey of Iran, Rep. No. **57**, p. 357-383 (1983).
12. Karimpour M.H. and Khin Z. Geochemistry and physicochemical condition of Qaleh-Zari Cu-Ag-Au ore bearing solution based on chlorite composition. *Iranian Journal of Crystallography and Mineralogy*, **8**: 3-22 (2000).
13. Hedenquist J.W. and Henley R.W. The important of CO_2 on freezing point measurements of fluid inclusion: evidence from active geothermal system and implication for epithermal ore deposition. *Econ. Geol.*, **80**: 1379-1406 (1985).
14. Bozzo A.T., Chen R. and Barduhn A.J. The properties of hydrates of chlorine and carbon dioxide. In: Delyannis A. and Delyannis E. (Eds.), fourth international symposium on fresh water from the sea, V. **3**: 437-451 (1973).
15. O'Neil J.R., Clayton R.N. and Mayeda T.K. Oxygen isotopes fractionation in divalent metal carbonates. *J. Chem. Phys.*, **51**: 5547-5558 (1969).
16. Ohmoto H. and Rye R.O. Isotopes of sulfur and carbon. In: Barnes H.L. (Ed.) *Geochemistry of Hydrothermal Ore Deposits*, Wiley, New York, pp. 509-567 (1979).
17. Taylor H.P. Oxygen and hydrogen isotopic studies of plutonic granitic rocks. *Earth Planet. Sci. Lett.*, **38**: 177-210 (1978).
18. Hassan Nejad A.A. and Moor F. The source of Qaleh Zari copper deposits with respect to new isotopic and fluid inclusion data. Proceeding of the 6th symposium of Geological Society of Iran, Kerman, Iran, 114-117 (2002).
19. Cathelineau M. and Nieva D. A chlorite solid solution geothermometer, the Los Azufres (Mexico) geothermal system. *Contrib. Mineral Petrol*, **19**: 235-244 (1985).
20. Walshe J.L. and Solomon M. An investigation into the environment of formation of the volcanic-hosted Mt. Lyell copper deposits, using geology, mineralogy, stable isotopes and a six component chlorite solid-solution model. *Econ. Geol.*, **76**: 246-238 (1981).
21. Walshe J.L. A six-component solid solution model and the conditions of chlorite formation in hydrothermal and geothermal systems. *Econ. Geol.*, **81**: 681-703 (1986).
22. Davies J. and Egerton P. The application of lithogeochemistry to gold exploration in the Casa Berardi area, northwestern Quebec. Doctoral Queen's University, Kingston, ON, Canada, p. 399 (1994).
23. Hammond N.Q. and Tabata H. Characteristics of ore minerals associated with gold at the Prestea mine. *Ghana. Mineralogical Magazine*, **61**(6): 879-894 (1997).
24. Huston D.L., Sie S.H., Suter G.F., Cooke D.R., Both R.A., and Walshe J.L. Trace elements in sulfide minerals from Eastern Australian volcanic hosted massive sulfide deposits. Part I. Proton Microprobe Analyses of Pyrite, chalcopyrite and Sphalerite. Part II. Selenium levels in Pyrite: comparison with D34S values and implications to the source of sulfur in volcanogenic hydrothermal systems. *Econ. Geol.*, **90**: 1167-1196 (1995).
25. Huston D.L., Sie S.H., Suter G.F. and Ryan C.G. The composition of pyrite in volcanogenic massive sulfide deposits as determined with the proton microprobe. *Nuclear Instruments and Methods in Physics Research*, **B75**: 531-533 (1993).
26. Simon G., Huang H., Penner-Hahn J., Kesler S.E., and Kao L.-S. Oxidation state of gold and arsenic in gold-bearing arsenian pyrite. *Am. Mineralogist*, **84**: 1071-1079 (1999).
27. Simon G., Kesler S.E., and Chryssoulis S. Geochemistry and textures of gold-bearing arsenian pyrite, Twin Creeks, Nevada: Implications for deposition of gold in Carlin-type deposits: *The Bulletin of the Society of Economic Geologists*, **94**(3): 405-421 (1999)**.**
28. Huston D.L., Sie S.H., and Suter G.F. Selenium and its importance to the study of ore genesis: the theoretical basis and its application to volcanic-hosted massive sulfide deposits using pixeprobe analysis. *Nuclear Instruments and Methods in Physics Research*, **B104**: 476-480 (1995).
29. Simon G., Kesler S.E., Essene E.J., and Chryssoulis S.L. Gold in porphyry copper deposits: Experimental determination of the distribution of gold in the Cu-Fe-S system at 400°C to 700°C. *Econ. Geol.*, **95**(2): 259-270 (2000).
30. Ohmoto H. Systematics of sulfur and carbon isotopes in hydrothermal ore deposits. *Ibid.*, **67**: 551-578 (1972).

Appendiex 1. Major and trace element content of volcanic rocks from Qaleh-Zari area [7]

Oxides %	**1**	**2**	**3**	**4**	**5**
SiO2	60.57	56.90	57.16	55.30	52.17
Al2O3	18.31	16.77	16.55	16.32	17.87
Fe2O3	3.38	5.34	5.34	5.41	3.37
FeO	1.52	2	2.13	2.13	4.93
MnO	0.18	0.24	0.13	0.16	0.15
MgO	0.80	3.43	3.48	2.73	4.35
CaO	3.85	6.69	5.97	7.29	8.30
Na_2O	2.81	2.08	2.53	2.36	2.03
K_2O	5.27	2.41	2.17	2.29	0.73
TiO_2	0.82	0.8	0.74	0.72	0.87
P_2O_5	0.19	0.15	0.19	0.19	0.21
H_2O^+	1.88	2.68	2.03	1.64	3.09
H_2O	0.27	0.14	0.21	0.35	0.25
CO_2	0.46	0.66	1.41	2.64	2.34
Trace (ppm)					
Cu	15	150	44	72	73
Pb	281	121	22	21	15
Zn	282	89	60	63	79
Rb	217	83	24	67	9
Sr	357	302	302	320	334
Ba	770	468	402	424	472
Ce	88	42	9	—	31

Appendix 2. Temperatures of homogenization and salinities of primary fluid inclusions from Stage I of mineralization (fluid inclusions in quartz are measured)

Vein	**Depth**	**Sample No.**	**Th°C* Range**	**Th°C Mean**	**T ice melting**	**Salinities** Range**	**Salinities Mean**
1	70	R-30	310-376	343	—	n.m	—
1	70	L-300	275-303	287	—	n.m	—
1	100	R-30	296-380	355	−1.45 to −2.1	2.5-3.4	3
1	135	R-100	300-335	315	−2.4 to −3.3	3.9-5.5	4.2
1	135	R-130	301-311	304	−1.8 to −3.4	3-5	3.6
1	170	R-30	312-343	318	−1.1 to −1.3	1.8-2.2	2
1	170	R-100	311-328	318	−3.2 to −3.5	5.3-5.5	5.4
2	70	R-30	280-357	350	—	n.m	—
2	100	L-100	314-338	322	−2.3 to −3.4	3.8-5.5	4.6
2	170	L-50	301-347	310	—	n.m	—
2	170	R-250	290-380	342	−2.3 to −2.4	3.8-4	3.9
3	70	L-50	270-287	284	—	n.m	—
3	100	L-50	298-324	309	—	n.m	—
3	100	L-100	270-316	298	—	n.m	—
3	100	R-50	296-344	314	−3.2 to −3.6	5.2-5.8	5.4
3	135	L-50	302-325	307	—	n.m	—
3	135	L-100	299-302	300	—	n.m	—

*Th = temperature of homogenization, **Salinities in wt % NaCl equiv, n.m.= not measured. Sample location (meter) from shaft No.1 (R) to the right and (L) to the left.

Appendix 3. Temperatures of homogenization and salinities of primary fluid inclusions from Stage II of mineralization (fluid inclusions in quartz are measured)

Vein	Depth	Sample No.	Th°C* Range	Th°C Mean	T ice melting	Salinities** Range	Salinities Mean
1	170	R-100 (qtz-py-het)	200-270	245	−2.8 to −3.2	4.5-5.2	4.9
1	170	R-100 (qtz-py)	287-298	295	—	n.m	—
1	170	R-30 (qtz-py-ccp-het)	282-304	303	−1.2 to −1.5	2.2-2.5	2.3
2	170	R-250 (qtz-py-ccp)	177-235	230	−1.2 to −2.1	2.3-3.4	2.9

*Th = temperature of homogenization, **Salinities in wt % NaCl equiv, n.m.= not measured. Sample location (meter) from shaft No.1 (R) to the right and (L) to the left.

Appendix 4. Temperatures of homogenization and salinities of primary fluid inclusions from Stage III and IV of mineralization (fluid inclusions in quartz are measured)

Vein	Depth	Sample No.	Mineral	Th°C* Range	Th°C Mean	T ice melting	Salinities** Range	Salinities Mean
2	100	L-100 stage III	Quartz	246-256	254	−1.1 to −1.3	1.8-2.3	2.1
2	100	L-50 Stage IV	Quartz	188-210	200	− 0.9 to −1.1	1.3-1.8	1.5

*Th = temperature of homogenization, **Salinities in wt % NaCl equiv. Sample location (meter) from shaft No.1 (R) to the right and (L) to the left.